第 48 卷 第 17 期/2021 年 9 月/中国激光 研究论文

中国激光

基于差分成像的激光光束指向性控制

杨红伟[1,2]，杜益冕[2]，吕立冬[2]，陶卫[1]，卢俊国[1]，赵辉[1*]

[1]上海交通大学电子信息与电气工程学院，上海 200240；

[2]安徽工业大学电气与信息工程学院，安徽 马鞍山 243032

摘要 激光光源的方向抖动是激光三角位移传感器测量误差的重要来源。为了抑制光源光束抖动，设计了一种基于差分成像的激光光束指向控制装置。该装置由一个准直激光器和两个接收透镜组组成，其中两个接收透镜组关于发射激光光束的光轴对称，每个接收透镜组由一个聚焦透镜和一个光电电荷耦合器件组成。激光光源光束抖动角度控制在 0.4°以内时，成像在两个光电探测器上的激光光束的质心的均值可控制在误差许可的范围内。实验结果表明，采用该装置，拟合误差的估计标准差由 28.53 μm 减小至 0.2532 μm，重复性精度由原来的±0.7 mm 降低至±5 μm，非线性误差由全量程的±0.8% 减小至全量程的±0.04%。

关键词 几何光学；激光三角位移传感器；激光光束指向性；差分成像

中图分类号 O436 **文献标志码** A **doi**：10.3788/CJL202148.1705002

1 引 言

激光三角位移传感器(LTDS)是一种高精度位移测量传感器，具有非接触测量、高精度、绝对测距等优点，广泛应用于机器人、精密加工制造、汽车电子等工业检测领域[1-9]。LTDS 的成像光路描述如下。准直激光器垂直投射准直激光光束至被测目标物上，形成的漫射光线经聚焦镜组聚焦后成像于光电耦合元件(CCD)上，定义 γ 为工作距离，α 为观测角，β 为成像角，l 和 l' 分别是聚焦镜组的物距和像距。当被测目标物沿垂直于激光光束光轴的方向移动时，成像于 CCD 上的成像像点亦随之移动。当被测目标物沿光轴移动距离 x 时，成像像点随之在 CCD 上移动 Δx。那么 x 与 Δx 之间呈近似线性关系[10-11]。依据 x 与 Δx 之间的几何关系便可以对被测目标物移动的位移进行标定。

随着激光加工技术的成熟，激光光束指向性趋于无限稳定。然而依据实验室测试数据，激光光束指向仍有±0.4°的抖动，激光光束指向抖动是光束切面质心的漂移。为抑制光源光束指向抖动对测量精度的影响，多篇文献中均提出了双光束成像并取成像位置均值的方法。Oh 等[12]提出了一种在聚焦镜组和 CCD 之间插入衍射光栅以在光电探测器上同时成多束波形的方法。Blais 等[13-14]提出了 Bi-Iris 方法，即在接收镜组的孔径处插入双孔径掩模，该技术可在 CCD 上双光束成像。Žbontar 等[15]采用投射圆环光源的方法取得对称的双高斯光束。文献[12-15]中的方法可减小电磁干扰、散斑、聚焦镜组的畸变和环境光的影响，然而由于双光束成像在同一侧，对抑制光源指向抖动带来的测量误差效果有限。Yang 等[16]设计了一种光源光束抖动抑制装置，该装置由三角棱镜、五角棱镜、半五角棱镜、双对称分束镜及两个斜方棱镜组成。基于该装置可得到对称差分的两束激光光束，因此无论光源如何抖动，差分的两束激光的质心的均值保持不变。此外，为克服该装置尺寸过大、棱镜的折射系数不等带来的测量误差及两束激光的峰值有数量级差异的问题，该团队改进了该装置。改进的装置由 5 片反射镜和 1 个双对称分束镜组成[17]。然而改进的装置因有诸如 157.5°、112.5°、22.5°的特殊角度，因此容易产生

收稿日期：2020-11-23；**修回日期**：2020-12-27；**录用日期**：2021-02-05

基金项目：国家自然科学基金(51977001)

通信作者：*huizhao@sjtu.edu.cn

安装误差。而且该误差与光源光束抖动的角度有关，无法通过标定的方法进行抑制。Ibaraki 等[18]给出了一种双视角结构，即对称的 2 个聚焦镜组和 2 个光电探测器分列于光源光轴的两侧，该结构可在 2 个光电探测器上成对称的两个像点。相较于文献[13]给出的单视角结构，文献[18]提出的结构不但可减小电磁干扰、散斑和镜头畸变带来的误差，还可对光源光束抖动产生的误差进行抑制。然而文献[18]给出的结构并不满足恒聚焦光路条件，因此会产生非线性误差。

本文基于文献[18-20]给出的双视角结构，提出了一种基于差分成像的光源指向稳定装置(DVLTDS)。该装置由对称的两个接收透镜组组成，其中接收透镜组由一个聚焦镜组和一个 CCD 组成，且接收透镜形成对称的两个恒聚焦光路。基于该装置，可在对称的两个 CCD 上同时生成对称的两个高斯波形，因此无论光源指向如何抖动，两束光的质心的均值保持不变。所提方法不但可抑制光源指向抖动，还可减小电磁干扰、散斑、聚焦镜组镜头畸变和环境光带来的测量误差。

2　基于差分成像的光束指向控制原理

DVLTDS 由准直激光器、对称于光源光轴的两个接收镜组组成，其中接收镜组由聚焦镜组和 CCD 组成。DVLTDS 的成像光路原理如图 1 所示，光源投射激光光点至被测目标物后生成差分的两束激光 P_1 和 P_2，两束激光分别经对称的两个聚焦镜组同时聚焦成像在对称的两个 CCD 上。

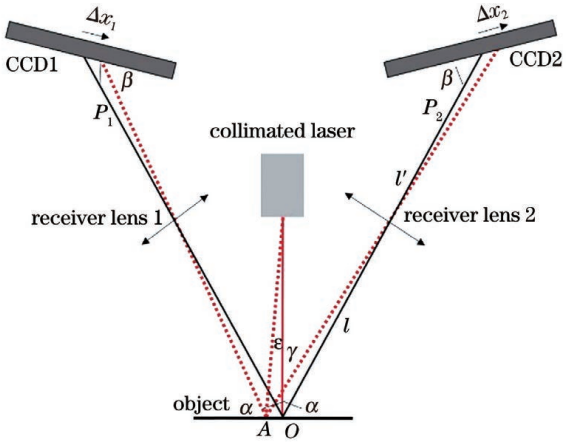

图 1　DVLTDS 光路原理

Fig. 1　Optical path principle of DVLTDS

从图 1 可以看出，当光源指向稳定时，差分光束 P_1 和 P_2 关于光源光轴对称，定义 x_1 和 x_2 分别为差分光束 P_1 和 P_2 的质心，那么均值 P_{os} 可写成为

$$P_{os}=\frac{x_1-x_2}{2}。\tag{1}$$

当光源光束抖动角度 ε 时，x_1 的变化量 Δx_1 为

$$\Delta x_1=\frac{l'}{l}\times\gamma\times\tan\varepsilon\times\frac{\cos Z_1}{\sin(\beta-Z_1+\alpha)},\tag{2}$$

式中：$Z_1=\arctan[(\gamma\cdot\tan\varepsilon+l\cdot\sin\alpha)/(l\cdot\cos\alpha)]$。

同理，x_2 的变化量 Δx_2 为

$$\Delta x_2=\frac{l'}{l}\times\gamma\times\tan\varepsilon\times\frac{\cos Z_2}{\sin(\beta-Z_2+\alpha)},\tag{3}$$

式中：$Z_2=\arctan[(-\gamma\cdot\tan\varepsilon+l\cdot\sin\alpha)/(l\cdot\cos\alpha)]$。

从图 1 可以看出，Δx_1 和 Δx_2 同向变化，因此依据(1)～(3)式，当光源光束抖动角度 ε 时，差分光束的质心的均值 P_v 为

$$P_v=\frac{(x_1+\Delta x_1)-(x_2+\Delta x_2)}{2}=P_{os}+E_{err},\tag{4}$$

其中

$$E_{err}=\frac{\Delta x_1-\Delta x_2}{2}=\frac{l'\gamma}{2l}\left[\frac{\cos Z_1}{\sin(\beta-Z_1+\alpha)}-\frac{\cos Z_2}{\sin(\beta-Z_2+\alpha)}\right]\cdot\tan\varepsilon。\tag{5}$$

由(5)式可知，如果 Z_1 和 Z_2 的值近似为零，E_{err} 亦近似为零，这意味着

$$\gamma\cdot\tan\varepsilon\ll l\cdot\sin\alpha。\tag{6}$$

因此，如果 γ、l、α 和 ε 的取值满足(6)式，无论光源指向如何抖动，P_{os} 与 P_v 总是近似相等，即差分光束的质心均值保持不变。

3　实验及结果

3.1　光路设计

依据实验室数据，抖动角度 ε 介于 −0.4°到 0.4°之间。为满足(6)式，聚焦镜组和 CCD 的位置需要详细设计。基于 Zemax 的非序列模式的光路设计如图 2 所示，其中聚焦镜组的焦距是 31.0788 mm，观测角 α 设置为 20.04°。

其他光学设计参数 l、l'、β 和 γ 的取值如表 1 所示。

表 1　光学设计参数值

Table 1　Values of parameters

Parameter	Value
l /mm	145.600
l' /mm	39.5149
β /(°)	53.36
γ /mm	79.5000

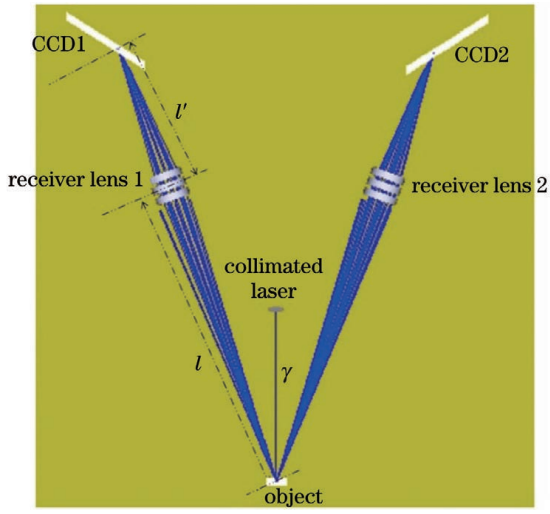

图 2　基于 Zemax 软件设计的 DVLTDS 模型

Fig. 2　DVLTDS model designed in Zemax software

由表 1 可知，$\gamma \cdot \tan\varepsilon$ 和 $l \cdot \sin\alpha$ 分别为 0.5550 mm 和 49.8936 mm，满足(6)式的要求。

3.2　标定实验

依据以上参数值搭建的 DVLTDS 装置如图 3 所示。该实验装置由 DVLTDS、标准陶瓷量块、旋转装置、一维线性移动平台和双频激光干涉仪(由 beam reducer、retro-reflector 和 laser head 组成)组成。

实验中采用的双频激光干涉仪(型号 XL-80，雷尼绍)精度为 1 nm，高出 LTDS 精度 3 个数量级，因此其测量值可作为标定测试、重复性测试和非线性测试的标准值。标准陶瓷量块和 beam reducer 同时固定在由步进电机驱动的一维线性移动平台上，步进电机驱动一维移动平台由近光点向远光点步进，步进范围为 0～10 mm，步幅为 0.1 mm。为描述方便，近光点和远光点的中点定义为零点。为模拟光源光束抖动角度，准直激光器由旋转装置驱动，在 −0.4°～0.4°变化。采用的主要装置如表 2 所示。

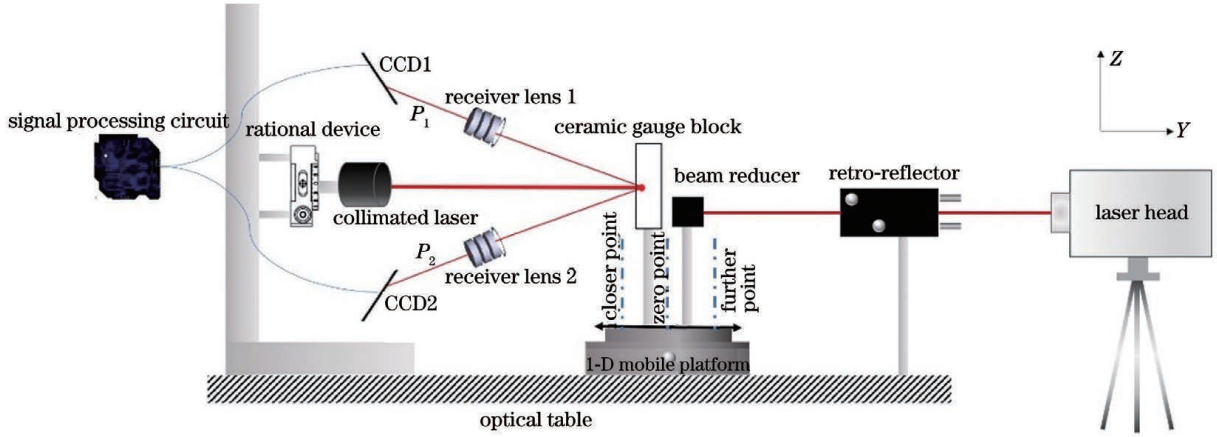

图 3　DVLTDS 实验装置

Fig. 3　Experimental device of DVLTDS

表 2　DVLTDS 中的主要器件

Table 2　Main devices used in DVLTDS

Device	Type	Parameter
CCD	TCD2566BFG	Resolution: 5.25 μm
Ceramic gauge block		Size: 20 mm×10 mm×2mm
Collimated laser		Power: 5 W
Receiver lens		Focus: 31.0788 mm
Rational device	PRM/M(Thorlab)	

为描述方便，将 receiver lens 2 和 CCD2 组成的结构定义为 LTDS，对激光光束 P_2 的标定结果进行对比。标定方法描述如下：由步进电机驱动的标准陶瓷量块在 0～10 mm 内运行，步幅设定为 0.1 mm；且在每个位置，准直激光光束的指向性在 −0.4°～0.4°内变化(间隔为 0.1°)。其中 P_v 值作为 DVLTDS 的标定基准，激光光束 P_2 的质心值作为未使用光束指向控制装置的 LTDS 的标定基准。

标定数据和标定误差分别如图 4 和图 5 所示。其中图 4(a)是 DVLTDS 的标定数据，图 4(b)是 LTDS 的标定数据。图 5(a)和图 5(b)分别为二者的标定误差，Pixel 是质心在 CCD 上的像素值。

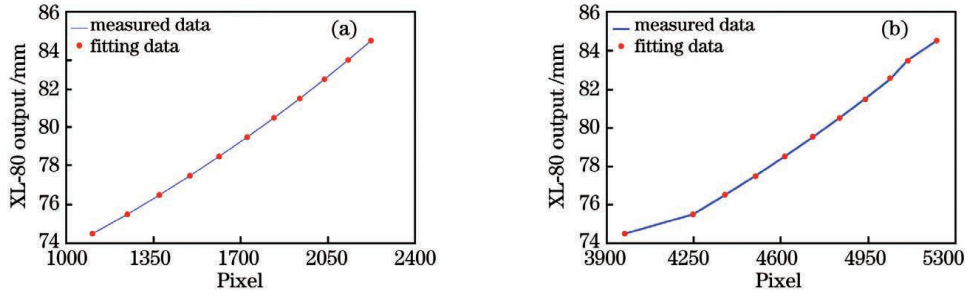

图 4　标定数据曲线。(a) DVLTDS 的标定结果；(b) LTDS 的标定结果

Fig. 4　Calibration data curve. (a) Calibration results of DVLTDS; (b) calibration results of LTDS

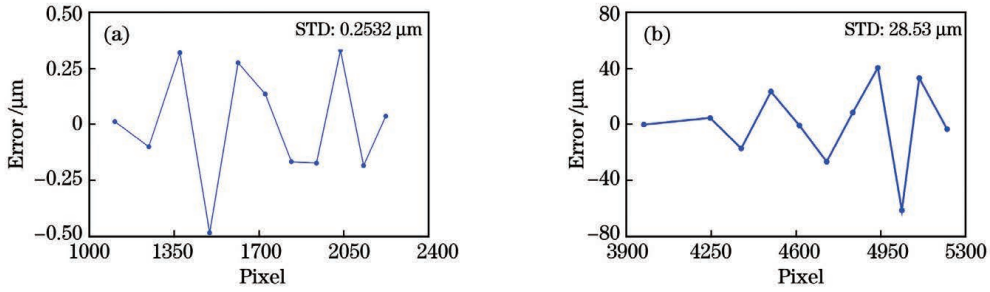

图 5　标定误差曲线。(a) DVLTDS 的标定误差；(b) LTDS 的标定误差

Fig. 5　Calibrated error curve. (a) Calibrated errors of DVLTDS; (b) calibrated errors of LTDS

由图 5(a)可知，进行光束指向控制后的装置 DVLTDS 的标准方差估计(STD)是 0.2532 μm。由图 5(b)可知，未进行光束指向控制的 STD 高达 28.53 μm，即基于 DVLTDS 的拟合曲线很好地跟随激光干涉仪得到的结果。

3.3　重复性测试

标准陶瓷量块分别固定于近光点、远光点和零点。当准直激光光束指向在−0.4°～0.4°内变化时(间隔为 0.1°)，基于 DVLTDS 和基于 LTDS 的重复性测试结果如图 6 所示。

由图 6(a)、(c)和(e)可知，随着光源光束抖动角度的增大，DVLTDS 的测量值先增大后降低，且抖动角度越接近 0°，测量误差越小，且重复性误差控制在 μm 级以内；由图 6(b)、(d)和(f)可知，未采用光束指向控制的 LTDS 的测量值随光源光束抖动角度的增大而呈现递减趋势，且重复性误差达 mm 级。当光源抖动在−0.4°～−0.2°变化时，远光点处的像点无法聚焦，因为在进行基于光强分布的质心计算时，出现了较大的计算误差，由此导致了图 6(f)中出现测量值先增大后递减的现象。尽管如此，总体上仍呈现与图 6(b)和图 6(d)相同的递减趋势。基于 DVLTDS 和基于 LTDS 的重复性误差及 STD 如表 3 所示。

表 3　近光点、零点和远光点的重复性误差和标准方差估计

Table 3　Repeatability error and STD at closer point, zero point, and further point

Position	Repeatability error /μm		STD /mm	
	DVLTDS	LTDS	DVLTDS	LTDS
Closer point	±4.6375	±1228.8	0.0035	0.8516
Zero point	±3.8836	±791.6	0.0030	0.9567
Further point	±4.3520	±1402.1	0.0034	0.5476

综合近光点、零点和远光点的重复性误差和 STD 的数据，全量程内未采用光束指向控制的 LTDS 的重复性误差和 STD 的最小值分别超过 ±0.7 mm 和 0.5 mm，而采用了光束指向控制的 DVLTDS 的重复性误差和 STD 分别减小至 ±5 μm 和 0.0035 mm 以内。

3.4　非线性测试

非线性定义为 $(x_t - x_r)/l_r$，其中 x_t 是由 LTDS 得到的测量值，x_r 是由激光干涉仪 XL-80 得到的标准值，l_r 为测量范围。在该实验中，标准陶瓷量块由步进电机驱动，由近光点移动到远光点，步幅为 0.1 mm，记录每个位置的测量值和XL-80得

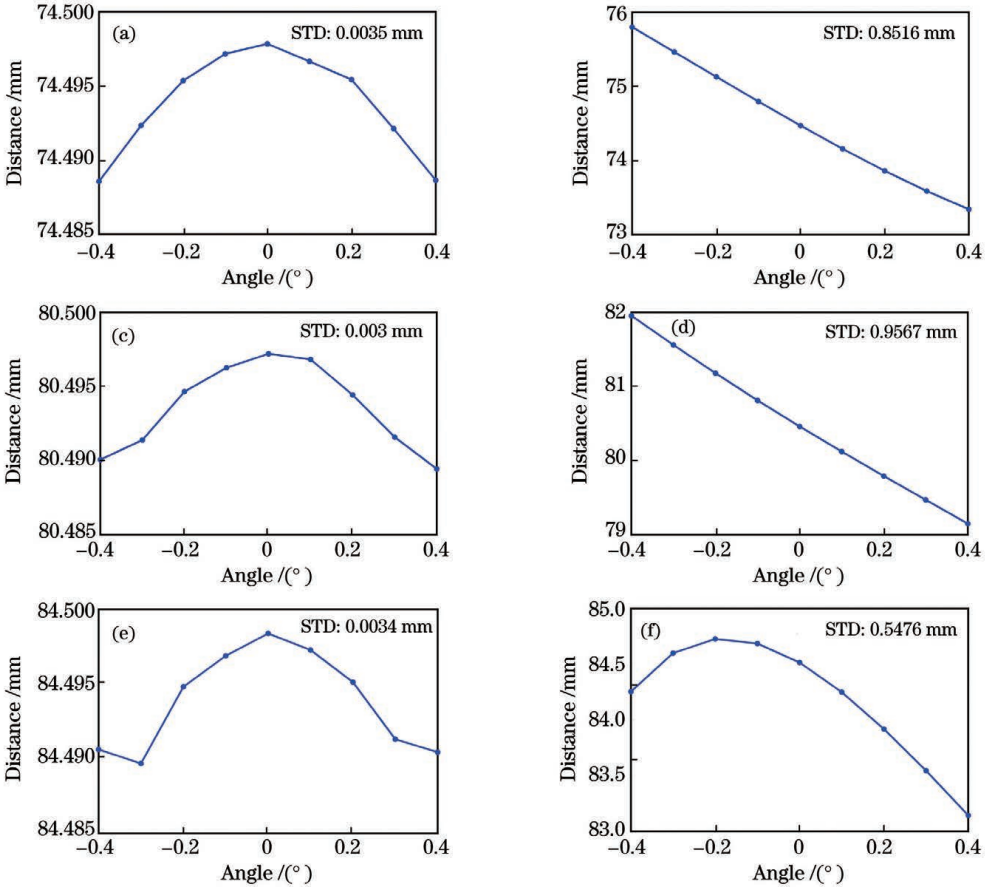

图 6　采用和未采用差分成像时近光点、零点和远光点的重复性曲线。(a)近光点处采用 DVLTDS 的重复性结果;(b) 近光点处采用 LTDS 的重复性结果;(c) 零点处采用 DVLTDS 的重复性结果;(d)零点处采用 LTDS 的重复性结果;(e) 远光点处采用 DVLTDS 的重复性结果;(f) 远光点处采用 LTDS 的重复性结果

Fig. 6　Repeatability curves at closer point, zero point, and further point with and without differential dual-view imaging. (a) Repeatability results with DVLTDS when the object is located at a closer point; (b) repeatability results with LTDS when the object is located at a closer point; (c) repeatability results with DVLTDS when the object is located at a zero point; (d) repeatability results with LTDS when the object is located at a zero point; (e) repeatability results with DVLTDS when the object is located at a further point; (f) repeatability results with LTDS when the object is located at a further point

到的标准值,并重复 3 次。DVLTDS 和 LTDS 得到的测试结果与激光干涉仪 XL-80 得到的测量值之间的误差($x_t - x_r$)如图 7 所示。由图 7(a)可知,DVLTDS 测得数据的非线性度为全量程的±0.04%;由图 7(b)可知,未采用光束指向控制的 LTDS 测得数据的非线性度达全量程的±0.8%。

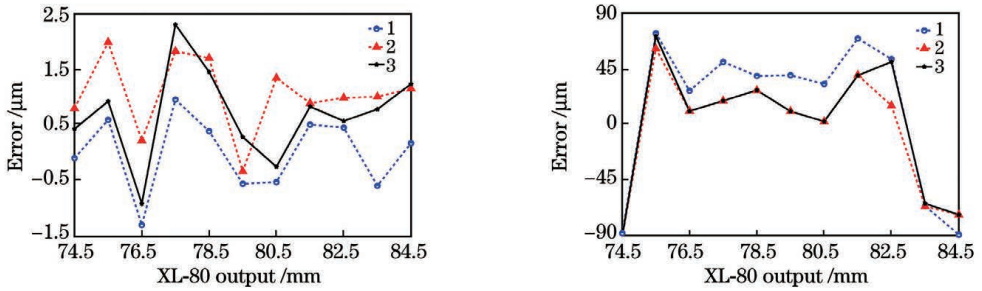

图 7　采用和未采用差分成像的非线性误差。(a) DVLTDS 的非线性误差;(b) LTDS 的非线性误差

Fig. 7　Nonlinearity errors with and without differential dual-view imaging. (a) Nonlinearity errors of DVLTDS; (b) nonlinearity errors of LTDS

4 结 论

光源指向抖动是激光检测中测量误差的重要来源之一。本文提出了一种基于差分成像的激光光源指向抖动控制装置，该装置由准直激光器、两个对称的聚焦镜组和 CCD 组成，可抑制光源光束抖动带来的测量误差。基于该装置，可在两个 CCD 上同时生成差分的激光光束，因此无论光源指向如何变化，成像在 CCD 上的两束激光的质心的均值均保持不变。实验结果表明：当光源指向由 −0.4°到 0.4°变化时，采用 DVLTDS 的非线性度优于全量程的 ±0.04%，单点重复性的 STD 优于 0.0035 mm；而未采用光源指向控制的传统 LTDS 的非线性度达全量程的 ±0.8%，单点重复性的 STD 高于 0.5mm。

参 考 文 献

[1] Dong Z X, Sun X W, Chen C Z, et al. An improved signal processing method for the laser displacement sensor in mechanical systems[J]. Mechanical Systems and Signal Processing, 2019, 122: 403-418.

[2] Li T, Xing Z Y, Chen S. An online wheel size detecting technology based on laser displacement sensors for urban rail vehicles [C]// 36th Chinese Control Conference (CCC), July 26-28, 2017, Dalian, China. New York: IEEE Press, 2017: 9983-9987.

[3] Sun J H, Zhang J, Liu Z, et al. A vision measurement model of laser displacement sensor and its calibration method [J]. Optics and Lasers in Engineering, 2013, 51(12): 1344-1352.

[4] Costa M F. Optical triangulation-based microtopographic inspection of surfaces[J]. Sensors, 2012, 12(4): 4399-4420.

[5] Cigada A, Mancosu F, Manzoni S, et al. Laser-triangulation device for in-line measurement of road texture at medium and high speed[J]. Mechanical Systems and Signal Processing, 2010, 24(7): 2225-2234.

[6] Zhang F M, Qu X H, Ouyang J F. An automated inner dimensional measurement system based on a laser displacement sensor for long-stepped pipes[J]. Sensors, 2012, 12(5): 5824-5834.

[7] Liu K M, Tao W, Chen X, et al. Laser triangulation method for glass thickness by automatically adapting to displacement change [J]. Chinese Journal of Lasers, 2020, 47(1): 0104003.

[8] Duan X D, Wu B, Kang J H. Calibration method for spatial pose of laser beam with high-accuracy[J]. Acta Optica Sinica, 2019, 39(8): 0812002.
段晓登, 吴斌, 康杰虎. 激光束空间位姿高精度标定方法[J]. 光学学报, 2019, 39(8): 0812002.

[9] Zhang T, Zhang M H, Zou Y B. Path planning of robot processing based on three-dimensional point cloud[J]. Chinese Journal of Lasers, 2018, 45(5): 0502009.
张铁, 张美辉, 邹焱飚. 基于三维点云的机器人加工轨迹规划[J]. 中国激光, 2018, 45(5): 0502009.

[10] Yang H W, Tao W, Liu K M, et al. Irradiance distribution model for laser triangulation displacement sensor and parameter optimization [J]. Optical Engineering, 2019, 58(9): 095106.

[11] Cui H, Guo R, Li X Q, et al. Calibration of laser triangular displacement sensor based on nonlinear fitting[J]. Chinese Journal of Lasers, 2020, 47(9): 0904003.
崔昊, 郭锐, 李兴强, 等. 基于非线性拟合的激光三角位移传感器标定方法[J]. 中国激光, 2020, 47(9): 0904003.

[12] Oh S, Kim K C, Kim S H, et al. Resolution enhancement using a diffraction grating for optical triangulation displacement sensors[J]. Proceedings of SPIE, 2001, 4285: 102-108.

[13] Blais F. Review of 20 years of range sensor development [J]. Journal of Electronic Imaging, 2004, 13(1): 231-243.

[14] Lang S, Korba L, Blais F, et al. Characterization and testing of the BIRIS range sensor[C]//1993 IEEE Instrumentation and Measurement Technology Conference, May 18-20, 1993, Irvine, CA, USA. New York: IEEE Press, 1993: 459-464.

[15] Žbontar K, Mihelj M, Podobnik B, et al. Dynamic symmetrical pattern projection based laser triangulation sensor for precise surface position measurement of various material types[J]. Applied Optics, 2013, 52(12): 2750-2760.

[16] Yang H W, Tao W, Zhang Z Q, et al. Reduction of the influence of laser beam directional dithering in a laser triangulation displacement probe[J]. Sensors, 2017, 17(5): E1126.

[17] Yang H W, Tao W, Yin X Q, et al. Differential correction system of laser beam directional dithering based on symmetrical beamsplitter [J]. Optical Review, 2018, 25(1): 10-17.

[18] Ibaraki S, Kitagawa Y, Kimura Y, et al. On the limitation of dual-view triangulation in reducing the measurement error induced by the speckle noise in scanning operations[J]. The International Journal of

Advanced Manufacturing Technology, 2017, 88(1/2/3/4): 731-737.

[19] Shiou F J, Liu M X. Development of a novel scattered triangulation laser probe with six linear charge-coupled devices (CCDs)[J]. Optics and Lasers in Engineering, 2009, 47(1): 7-18.

[20] Taylor J, Beraldin J A, Godin G, et al. NRC 3D imaging technology for museum and heritage applications[J]. The Journal of Visualization and Computer Animation, 2003, 14(3): 121-138.

Laser Beam Pointing Control Based on Differential Dual-View Imaging

Yang Hongwei[1,2], Du Yimian[2], Lü Lidong[2], Tao Wei[1], Lu Junguo[1], Zhao Hui[1*]

[1] *School of Electronic Information and Electrical Engineering, Shanghai Jiao Tong University, Shanghai* 200240, *China*;

[2] *School of Electrical and Information Engineering, Anhui University of Technology, Ma'anshan, Anhui* 243032, *China*

Abstract

Objective As a displacement measurement tool, laser triangulation displacement sensors (LTDS) are widely used in industrial detection because of their noncontact nature and high accuracy. The optical path of LTDS is illustrated as follows: a collimated laser beam is projected onto the detected object and the diffuse reflected light is focused by a receiver lens onto a charge-coupled device (CCD) detector. When the detected object is moved along the direction perpendicular to the optical axis of the source laser beam, the reflected light beam spot (image spot) focused on the CCD will move correspondingly. Thus, the displacement over which the detected object moves can be calculated using a geometric optical model that is related to the image spot displacement. Laser-beam dithering is considered one of the major error sources in laser applications. To solve this problem, many averaging methods have been proposed. However, methods that can image two image spots on one CCD with a single image system are ineffective at improving the error factor of the laser beam directional instability. In other methods, structures comprising prisms or reflectors for producing two differential optical paths have been proposed. With those methods, the positional average of two image spots remains constant irrespective of the angle by which the source laser beam dithers. However, an installation error might be introduced, for which calibration is not possible because it is related to the laser dithering angle.

Methods In this paper, a laser beam pointing control-based dual-view for laser triangulation displacement sensors (DVLTDS) is proposed. The structure comprises a collimated laser, two receiver lenses, and two CCDs, where the two receiver lenses and two CCDs are symmetrically arranged around to the optical axis of the source laser beam. DVLTDS generates two beam intensity distributions (BIDS) on two CCDs simultaneously. It converts the centroid movement of each BID into the detected object displacements through averaging. Hence, if the relationship among the optical parameters such as object distance, image distance, view angle, image angle, working distance, and the dithering angle satisfies certain constraint conditions (Eq. 6), then at the angle at which the source laser beam dithers, the average positions of the two laser spots imaged on the two detectors are equal within the permissible error range.

Results and Discussions For validating DVLTDS, an experimental setup was built and various tests, including calibration, repeatability, and nonlinearity, were conducted. To satisfy the constraint condition, the optical parameters, including the focus of the receiver lens, working distance, object distance, image distance, view angle, and image angle, were designed in Zemax software in the nonsequential mode (Fig. 2). The experimental platform of DVLTDS was built according to the design data (Table 1, Fig. 3).

DVLTDS was calibrated with a dual-frequency laser interferometer (RENISHAW XL-80) with a linear resolution of 1 nm. The relative positions of DVLTDS were calibrated. The target object (a ceramic block) was driven point-by-point along the optical axis of the source laser beam using a stepper motor with an increment of 0.1 mm within 10 mm. At each point, the collimated red laser was rotated with an increment of 0.1° within ±0.4°. Results show that the calibration curve of DVLTDS was coincident with that of the laser interferometer. Moreover, the standard deviation (STD) was found to be 0.2532 μm with DVLTDS [Fig. 5(a)]. In comparison, the STD was found to be 28.53 μm with LTDS [Fig. 5(b)].

In repeatability tests, the ceramic block was fixed at a closer point, zero point, and a farther point. The collimated red laser was rotated within $\pm 0.4^{\circ}$ with an increment of 0.1°. Using DVLTDS, the repeatability accuracy was within ± 5 μm and the STD was within 0.0035 mm. In comparison, with LTDS, the repeatability accuracy was ± 1.4 mm and the STD was more than 0.5 mm (Table 3).

The nonlinearity is expressed as the ratio of l_r to $(x_t - x_r)$, where x_t is the tested value of DVLTDS, x_r is the tested value of the XL-80 interferometer, and l_r is the tested range. In this experiment, measurements were performed by moving objects from a closer point to a farther point with an increment of 0.1 mm for three runs. The results reveal that the nonlinearity of DVLTDS is within $\pm 0.04\%$ full scale (F.S.) [Fig. 7(a)]. In comparison, the nonlinearity without differential dual view is within $\pm 0.8\%$ F.S. [Fig. 7(b)].

Conclusions In conclusion, experimental results indicate that with DVLTDS, the estimated STD of the fitting error decreases from 28.53 to 0.2532 μm, the repeatability accuracy can be reduced from ± 1.4 to ± 5 μm, and the nonlinear error can be reduced from $\pm 0.8\%$ F.S. to $\pm 0.04\%$ F.S. These results verify that laser beam pointing control-based dual-view for laser displacement sensors can suppress the effects of laser beam dithering.

Key words geometric optics; laser triangulation displacement sensor; laser beam directivity; differential imaging

OCIS codes 080.2740; 040.1880; 120.1880; 120.4570